AMERICAN SOCIETY FOR MICROBIOLOGY | Journal of Virology

Abelson Kinase Inhibitors Are Potent Inhibitors of Severe Acute Respiratory Syndrome Coronavirus and Middle East Respiratory Syndrome Coronavirus Fusion

Christopher M. Coleman,[a] Jeanne M. Sisk,[a] Rebecca M. Mingo,[b] Elizabeth A. Nelson,[b] Judith M. White,[b] Matthew B. Frieman[a]

Department of Microbiology and Immunology, University of Maryland, Baltimore, Maryland, USA[a]; Department of Cell Biology, University of Virginia, Charlottesville, Virginia, USA[b]

ABSTRACT

The highly pathogenic severe acute respiratory syndrome coronavirus (SARS-CoV) and Middle East respiratory syndrome coronavirus (MERS-CoV) cause significant morbidity and morality. There is currently no approved therapeutic for highly pathogenic coronaviruses, even as MERS-CoV is spreading throughout the Middle East. We previously screened a library of FDA-approved drugs for inhibitors of coronavirus replication in which we identified Abelson (Abl) kinase inhibitors, including the anticancer drug imatinib, as inhibitors of both SARS-CoV and MERS-CoV *in vitro*. Here we show that the anti-CoV activity of imatinib occurs at the early stages of infection, after internalization and endosomal trafficking, by inhibiting fusion of the virions at the endosomal membrane. We specifically identified the imatinib target, Abelson tyrosine-protein kinase 2 (Abl2), as required for efficient SARS-CoV and MERS-CoV replication *in vitro*. These data demonstrate that specific approved drugs can be characterized *in vitro* for their anticoronavirus activity and used to identify host proteins required for coronavirus replication. This type of study is an important step in the repurposing of approved drugs for treatment of emerging coronaviruses.

IMPORTANCE

Both SARS-CoV and MERS-CoV are zoonotic infections, with bats as the primary source. The 2003 SARS-CoV outbreak began in Guangdong Province in China and spread to humans via civet cats and raccoon dogs in the wet markets before spreading to 37 countries. The virus caused 8,096 confirmed cases of SARS and 774 deaths (a case fatality rate of ~10%). The MERS-CoV outbreak began in Saudi Arabia and has spread to 27 countries. MERS-CoV is believed to have emerged from bats and passed into humans via camels. The ongoing outbreak of MERS-CoV has resulted in 1,791 cases of MERS and 640 deaths (a case fatality rate of 36%). The emergence of SARS-CoV and MERS-CoV provides evidence that coronaviruses are currently spreading from zoonotic sources and can be highly pathogenic, causing serious morbidity and mortality in humans. Treatment of SARS-CoV and MERS-CoV infection is limited to providing supportive therapy consistent with any serious lung disease, as no specific drugs have been approved as therapeutics. Highly pathogenic coronaviruses are rare and appear to emerge and disappear within just a few years. Currently, MERS-CoV is still spreading, as new infections continue to be reported. The outbreaks of SARS-CoV and MERS-CoV and the continuing diagnosis of new MERS cases highlight the need for finding therapeutics for these diseases and potential future coronavirus outbreaks. Screening FDA-approved drugs streamlines the pipeline for this process, as these drugs have already been tested for safety in humans.

The severe acute respiratory syndrome (SARS) and Middle East respiratory syndrome (MERS) coronaviruses (CoVs) are two highly pathogenic viruses that infect humans. These viruses undergo a distinct replication cycle, involving virion entry, RNA genome replication and transcription of viral mRNAs, protein translation, virion assembly in the endoplasmic reticulum (ER)-Golgi intermediate complex, and egress by exocytosis of assembled virions (reviewed in reference 1). Coronavirus entry can be further subdivided into virion binding, receptor-mediated endocytosis, intracellular trafficking, and protease-dependent cleavage of spike (S) protein, leading to fusion of the virion membrane to the endosomal membrane. The SARS-CoV virion is endocytosed following S binding to angiotensin-converting enzyme 2 (ACE2) and trafficking to the late endosome, where the virion membrane fuses with the endosomal membrane in a cathepsin L-dependent manner (2). The MERS-CoV virion is endocytosed following S binding to dipeptidyl peptidase 4 (DPP4) and trafficking to the early endosome, where the virion membrane fuses with the endosomal membrane in a furin-dependent manner (3).

The outbreaks of SARS-CoV and MERS-CoV highlight the need to find treatments for these and potential future coronavirus outbreaks. The drug development process from novel compound to approved drug generally takes over 10 years, making it impractical to develop novel anticoronavirus drugs once an outbreak begins. For SARS-CoV, drugs that inhibit the viral protease (4–7), replicase (8–10), or helicase (10, 11) *in vitro* have been identified;

Received 18 July 2016 **Accepted** 18 July 2016

Accepted manuscript posted online 27 July 2016

Citation Coleman CM, Sisk JM, Mingo RM, Nelson EA, White JM, Frieman MB. 2016. Abelson kinase inhibitors are potent inhibitors of severe acute respiratory syndrome coronavirus and Middle East respiratory syndrome coronavirus fusion. J Virol 90:8924–8933. doi:10.1128/JVI.01429-16.

Editor: S. López, Instituto de Biotecnologia/UNAM

Address correspondence to Matthew B. Frieman, mfrieman@som.umaryland.edu.

C.M.C. and J.M.S. contributed equally to this article.

however, none have been approved for use in humans or have shown efficacy against SARS-CoV in animal models (12). An alternative approach to novel drug design is to screen FDA-approved drugs to determine their anticoronavirus activity, as these have already undergone safety testing and can be used in humans quickly with known safety profiles.

A previous study of FDA-approved drugs identified imatinib, an Abelson (Abl) kinase inhibitor, as a potent inhibitor of both SARS-CoV and MERS-CoV (13). Abl kinases are reversible nonreceptor tyrosine kinases that regulate several cellular pathways, including cell migration, adhesion, and actin reorganization. In mammals, there are two Abl kinases, Abl1 (Abl in mice) and Abl2 (Arg in mice). Abl kinase inhibitors have previously been shown to inhibit replication of Ebola virus (14, 15), coxsackievirus (16), and vaccinia virus (17), but at different points of the virus life cycle. Here, we used live virus and pseudotyped virions to determine precisely which steps in the SARS-CoV and MERS-CoV life cycles are inhibited by imatinib. We demonstrate that imatinib inhibits both SARS-CoV and MERS-CoV replication by a novel mechanism of blocking coronavirus virion fusion with the endosomal membrane. We also show that of the canonical imatinib targets, Abl2, but not Abl1, is required for SARS-CoV and MERS-CoV replication. These data suggest that Abl2 plays a role in coronavirus replication and that the inhibition of entry by imatinib is through inhibition of Abl2 kinase activity. Our results also demonstrate that a drug from a SARS-CoV and MERS-CoV drug screen could be used as a probe to identify host proteins responsible for coronavirus replication.

MATERIALS AND METHODS

Cells, viruses, and plasmids. HEK293T cells (human embryonic kidney cell line, ATCC CRL-3216) and Huh-7 cells (human hepatocarcinoma cell line, kindly provided by Reed Johnson [NIH]) were grown in high-glucose Dulbecco's modified Eagle's medium (DMEM) (Gibco) supplemented with 10% (vol/vol) fetal bovine serum (FBS) (Gibco), 1% L-glutamine (Gibco), and 1% penicillin-streptomycin (Gemini Bio-Products) at 37°C in a 5% CO_2 atmosphere. Vero E6 cells (monkey kidney epithelial cells, ATCC CRL-1586), MRC5 cells (human lung fibroblast cell line, ATCC CCL-171), and BSC1 cells (monkey kidney epithelial cells, ATCC CCL-26) were grown in minimal essential medium (MEM) (Corning) supplemented with 10% (vol/vol) FBS (Sigma-Aldrich), 1% L-glutamine (Gibco), and 1% penicillin-streptomycin (Gemini Bio-Products) at 37°C in a 5% CO_2 atmosphere.

SARS-CoV (strain MA15) is a mouse-adapted SARS-CoV strain containing 6 amino acid mutations compared to wild-type SARS-CoV (Urbani) as previously characterized (18, 19). The Jordan MERS-CoV strain (GenBank accession no. KC776174.1, MERS-CoV Hu/Jordan-N3/2012) was kindly provided by Kanta Subbarao (National Institutes of Health, Bethesda, MD), Gabriel Defang (Naval Medical Research Unit-3 [NAMRU-3], Cairo, Egypt) Michael Cooper (Armed Forces Health Surveillance Center), and Emad Mohereb (NAMRU-3). SARS-CoV and MERS-CoV virus stocks were grown and quantified as described previously (20). All work with live SARS-CoV or MERS-CoV was performed under biosafety level 3 conditions at the University of Maryland School of Medicine.

Pseudotyping plasmids. Human immunodeficiency virus (HIV) pseudotyping plasmids Δ8.2 (HIV genome containing Env mutation) and pMM310 (vpr-BlaM) were kindly provided by C. Broder (Uniformed Services University of the Health Sciences). The SARS S19 plasmid was kindly provided by Shutoku Matsuyama and Fumihiro Taguchi (NIID, Tokyo, Japan). A codon-optimized sequence for MERS S (EMC strain), with a V5 epitope tag at its C terminus, was synthesized by Genescript, and the coding sequence was then subcloned into the pCAGGS expression vector using appended EcoRI and BglII restriction sites.

Imatinib time-of-addition experiments on infectious SARS-CoV and MERS-CoV production. Vero E6, MRC5, or Calu-3 cells were seeded into 24-well plates and cultured overnight. To assess the effect of imatinib on SARS-CoV and MERS-CoV entry, cells were prechilled at 4°C for 30 min, infected with 850 50% tissue culture infective doses ($TCID_{50}$) of either SARS-CoV or MERS-CoV, and adsorbed to the cell surface for 1 h at 4°C. Cells were then washed once in phosphate-buffered saline (PBS) (Quality Biological Inc.), imatinib (Cell Signaling), or dimethyl sulfoxide (DMSO) vehicle control (Sigma-Aldrich) was added, and the cells were cultured for 4 h at 37°C in 5% CO_2. Cells were then washed once in PBS, and normal growth medium was added and left for the remainder of the infection, i.e., 24 h for SARS-CoV (MA15) or 48 h for MERS-CoV (Jordan), when supernatants were collected to assess infectious virus titer by $TCID_{50}$ assay as previously described (20).

To assess the effect of imatinib on postentry steps of the SARS-CoV or MERS-CoV replication cycle, cells were infected with 850 $TCID_{50}$ of either SARS-CoV (MA15) or MERS-CoV (Jordan) for 5 h. Cells were then washed once in PBS, and imatinib or the DMSO control was added to the infected cells. At 24 h postinfection for SARS-CoV (MA15) or 48 h postinfection for MERS-CoV (Jordan), supernatants were collected to assess infectious virus titers by $TCID_{50}$ assay, as previously described (20).

Effect of imatinib on SARS-CoV and MERS-CoV RNA production. Vero E6 cells were seeded into 24-well plates and cultured overnight. Cells were prechilled at 4°C for 30 min, and then 850 $TCID_{50}$ of either SARS-CoV or MERS-CoV was allowed to adsorb to the cell surface for 1 h at 4°C. Cells were washed once in PBS and then either treated with imatinib and moved to 37°C in 5% CO_2 immediately or cultured for 4 h at 37°C in 5% CO_2 and then treated with imatinib.

After 12 h of infection, RNA was extracted from cells using TRIzol reagent (Ambion) and phenol-chloroform extraction according to the manufacturer's instructions. Levels of MERS-CoV UpE, M mRNA, and a transferrin receptor (TRFC) endogenous control were assessed as previously described (20). Following a cDNA synthesis using RevertAid reverse transcriptase (RT) (Thermo Scientific) according to the manufacturer's instructions, levels of SARS-CoV pp1a, N mRNA, and a GAPDH (glyceraldehyde-3-phosphate dehydrogenase) endogenous control were assessed as previously described (21).

PS/SARS-S and PS/MERS-S production. HIV pseudovirions were prepared essentially as described by Mingo et al. (22). HEK293T cells were seeded into 10-cm plates (Corning) and cultured overnight at 37°C in 5% CO_2. The next day, 9 ml of fresh medium (DMEM supplemented with 10% supplemented calf serum (SCS), 1% penicillin-streptomycin, 1% L-glutamine, 1% sodium pyruvate, and 0.01% active G418) was added. Cells were transfected using the calcium phosphate method. Briefly, equal volumes of 2× transfection buffer (50 mM HEPES, 180 mM NaCl, and 2 mM Na_2HPO_4 in H_2O) and DNA mixture (10 μg of each plasmid DNA [pMM310, Δ8.2, and SARS-S or MERS-S]) and 50 μl of NTE buffer (1.5 M NaCl, 100 mM Tris [pH 7.4], 10 mM EDTA [pH 8.0], and H_2O to 500 μl) were added together and incubated for 15 min. One milliliter of transfection buffer-DNA mixture was added dropwise to each plate, and cells were incubated for 48 h at 37°C in 5% CO_2. Supernatants were cleared twice by centrifugation at 1,070 × *g* for 10 min at 4°C. Pseudovirions (named PS/SARS-S for SARS-CoV S pseudovirions and PS/MERS-S for MERS-CoV S pseudovirions) were layered onto a sucrose cushion (20 mM HEPES, 20 mM morpholineethanesulfonic acid [MES], 130 mM NaCl, 20% sucrose, pH 7.4), centrifuged 2 h at 112,398 × *g* at 4°C, resuspended in 250 μl of sucrose buffer, and stored overnight on ice at 4°C then at −80°C for long-term storage.

Intracellular trafficking assay. Huh-7 cells (3×10^4 per well) or BSC-1 cells (1.25×10^5 per well) (for MERS-CoV and SARS-CoV pseudotyped viruses, respectively) or Vero cells (1×10^5 per well) (for live SARS-CoV and MERS-CoV) were plated on coverslips in 24-well plates

and cultured overnight at 37°C in 5% CO_2. Eighteen to 24 hours later, cells were pretreated for 1 h with pretreatment buffer (PTB), which consisted of 10 μM imatinib (Cell Signaling) diluted in Opti-MEM (Life Technologies). Cells were placed on ice for 15 min, and 100 μl of fresh cold PTB containing PS/SARS-S or PS/MERS-S pseudovirions or live SARS-CoV or MERS-CoV was added. Cells were spinoculated at 250 × *g* for 30 min at 4°C. PTB containing virions was replaced with fresh PTB, and cells were incubated at 37°C for up to 2 h. PTB was removed, and cells were fixed with 4% paraformaldehyde (PFA) for 15 min and then washed in PBS. Cells were incubated in blocking and permeabilization buffer (10% FBS, 0.05% saponin, 10 mM glycine, and 10 mM HEPES in PBS, pH 7.4) for 30 min. Antibodies were used to detect SARS S (ATCC), MERS S (kindly provided by Ralph Baric [University of North Carolina]), Lamp-1 (Developmental Studies Hybridoma Bank H4A3), and EEA-1 (Cell Signaling, 3288). Secondary antibodies used were anti-mouse–fluorescein isothiocyanate (FITC) (Sigma, F0257) and anti-rabbit–FITC (Vector Laboratories, FI-1000) and anti-mouse–Alexa 633 (Invitrogen, A21052) and anti-rabbit–Alexa 633 (Invitrogen, A21071). All antibodies were used at a 1:1,000 dilution. For live virus experiments, cells also were fixed after secondary antibody staining for 24 h in 4% PFA at 4°C prior to imaging. Imaging was performed using the Meta510 confocal microscope in the University of Maryland, Baltimore, confocal microscope core facility. Image files were analyzed with Image J Colocalization Finder. The particle size threshold was set for endosomes and virions using the "Analyze Particles" tool, and the same settings were used throughout analyses for counting the number of particles. Values for colocalization between both virus and vesicle markers were then produced. Percent virion/endosome colocalization using the Image J Colocalization Finder was graphed as percent compared to nonlocalized virions.

Fusion/entry assay. The pseudovirion entry assay was performed essentially as described by Mingo et al. (22). Briefly, 3×10^4 Huh-7 or 2×10^4 BSC cells per well were plated in 24-well or 96-well plates, respectively, and 24 h later, cells were pretreated and infected as described above for the trafficking assay. After infection, cells were incubated for 3 h at 37°C in 5% CO_2. PTB was removed, and cells were washed with loading buffer (LB) (47 ml clear DMEM, 5 mM probenecid, 2 mM L-glutamine, 25 mM HEPES, 200 nM bafilomycin, 5 μM E64d) and incubated for 1 h in the dark in CCF2 solution (LB, CCF2-AM, solution B [CCF2-AM kit K1032] [Thermo Fisher]). Cells were washed once with LB and incubated for 6 h to overnight with 10% FBS in LB. Percent CCF2 cleavage was assessed by flow cytometry on an LSRII instrument (Becton Dickinson) in the flow cytometry core facility at the University of Maryland, Baltimore. Data were analyzed using FlowJo.

Abl1 and Abl2 siRNA knockdown and Western blots. Vero E6 cells were transfected with specific Smartpool small interfering RNAs (siRNAs) against Abl1 or Abl2 or a scrambled siRNA control (Dharmacon) using Lipofectamine RNAiMAX transfection reagent (Sigma-Aldrich) according to the manufacturer's instructions. In both cases, transfected cells were left for 48 h and then infected with 85 $TCID_{50}$ of either SARS-CoV (MA15) or MERS-CoV (Jordan), and supernatants and TRIzol extracts were collected at 18 h postinfection for SARS-CoV or at 18 h and 48 h postinfection for MERS-CoV. Levels of Abl1 and Abl2 were assessed by Western blotting using anti-cAbl (Thermo Scientific) or anti-Abl2 (a kind gift from Peter Davies) antibodies, respectively.

Statistics. Statistical analyses were performed using one-way analysis of variance (ANOVA) and Tukey's multiple-comparison tests or the two-tailed Student *t* test using the GraphPad Prism online software package version 5. A *P* value of <0.05 was considered statistically significant.

RESULTS

Imatinib inhibits production of infectious SARS-CoV and MERS-CoV. We have previously shown that imatinib significantly inhibits SARS-CoV and MERS-CoV replication *in vitro* (13). In this study, we sought to identify where specifically in the coronavirus life cycle imatinib was inhibiting replication by treating cells with imatinib for either the first 4 h of infection or 5 h after infection. We performed the experiments in Vero E6 cells (for SARS-CoV and MERS-CoV), Calu-3 cells (for SARS-CoV), and MRC5 cells (for MERS-CoV).

When imatinib was added for the first 4 h of infection in Vero E6 cells, SARS-CoV (Fig. 1A, triangles) and MERS-CoV (Fig. 1B, triangles), we found that virus production, as quantified by $TCID_{50}$, was significantly inhibited in a dose-dependent manner. However, when imatinib was added at 5 h postinfection, levels of SARS-CoV (Fig. 1A, squares) and MERS-CoV (Fig. 1B, squares) virion production, as quantified by $TCID_{50}$, were significantly higher than when the drug was added before infection. For example, when 10 μM imatinib was added for the first 4 h of infection, MERS-CoV production was inhibited 50-fold (Fig. 1A, triangles) (5.2% ± 0.95% of untreated control level; $P < 0.05$), however, when imatinib was added at 5 h postinfection, MERS-CoV production was not inhibited (Fig. 1A, squares) (105% ± 4.07% of control level; $P > 0.05$).

To make sure that the inhibition of virus replication was not due to cell type specificity of a host pathway, we tested whether there was a time- and dose-dependent effect of imatinib on SARS-CoV and MERS-CoV production in Calu-3 and MRC5 cells. We found that the inhibition is not unique to Vero E6 cells, as SARS-CoV and MERS-CoV production was also inhibited when imatinib was added during the first 4 h of infection, but not when added at 5 h postinfection, in Calu-3 (Fig. 1C) or MRC5 (Fig. 1D) cells, respectively. These data suggest that imatinib inhibits a step in the SARS-CoV and MERS-CoV replication cycles that occurs within the first 4 h and no later than 5 h postinfection.

Imatinib inhibits SARS-CoV and MERS-CoV replication prior to RNA production. Coronavirus RNA replication begins after virion entry, and uncoating and can be detected as early as 6 h postinfection. Therefore, we investigated the effect of imatinib on SARS-CoV and MERS-CoV RNA production. We used primers targeted to SARS-CoV or MERS-CoV genomic RNA (pp1a and UpE, respectively) to assess total RNA levels and also primers to specific mRNAs of the SARS-CoV or MERS-CoV mRNA (UpE) to assess transcription.

Vero E6 cells were treated with imatinib before infection with either SARS-CoV or MERS-CoV (Fig. 2). RNA was harvested at 12 h postinfection and assessed for genomic RNA and mRNA expression. We found that imatinib significantly inhibited the production of both SARS-CoV and MERS-CoV genomic RNA (pp1a) (Fig. 2A and C, squares, respectively) and mRNA (Fig. 2B and D, squares, respectively) when added at the time of virion entry. However, when entry was allowed to proceed as normal and imatinib was added at 4 h postinfection, there was no significant effect on SARS-CoV and MERS-CoV genomic RNA (Fig. 2A and C, triangles, respectively) or mRNA (Fig. 2B and D, triangles, respectively). For example, at 25 μM imatinib, SARS-CoV genome RNA was inhibited 1,000-fold (0.1% ± 0.4% of untreated control value; $P < 0.05$) when imatinib was added for the first 4 h of infection (Fig. 2A, squares); however, when the drug was added at 5 h postinfection (Fig. 2A, triangles), SARS-CoV genome RNA production was not significantly inhibited (110% ± 7.2% of control value; $P > 0.05$).

These data demonstrate that if imatinib is given after coronavirus genomic RNA entry into the cytoplasm, there is no signifi-

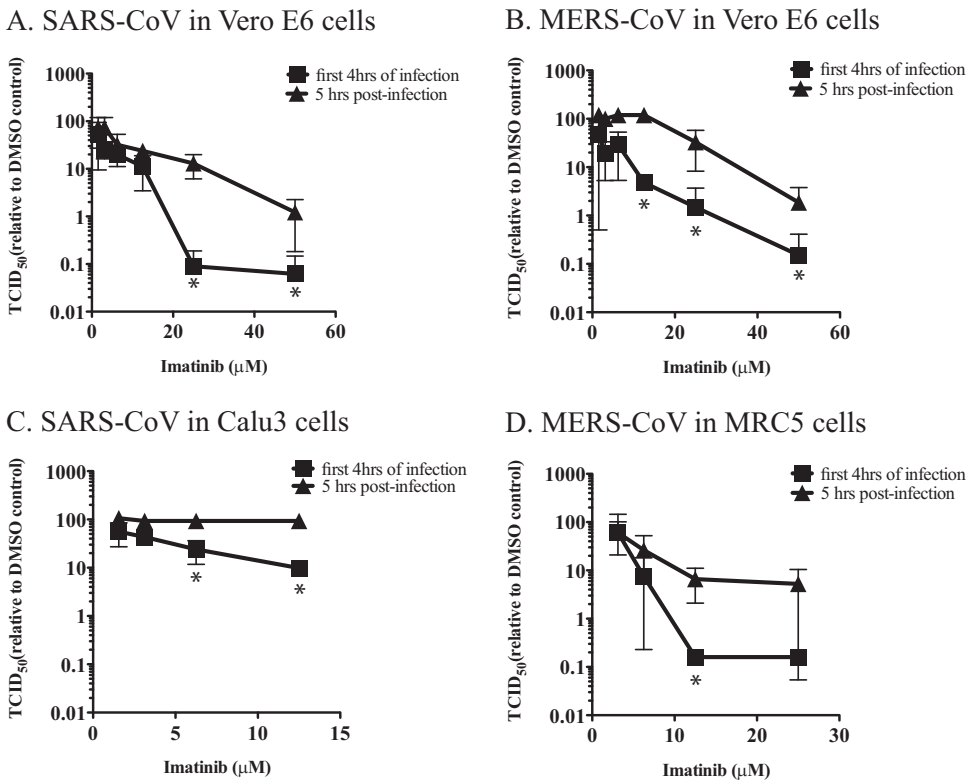

FIG 1 Imatinib inhibits SARS-CoV and MERS-CoV replication. Cells were treated with imatinib for the first 4 h (squares) or at 5 h postinfection (triangles) in all cases. Imatinib significantly inhibits SARS-CoV in Vero E6 (A) and Calu-3 (B) cells and MERS-CoV in Vero E6 (C) and MRC5 (D) cells when added for the first 4 h of infection but has a significantly diminished effect when added at 5 h postinfection. Data are presented as the mean ± standard deviation from 3 independent experiments. *, $P < 0.05$; **, $P < 0.01$.

cant inhibition of SARS-CoV and MERS-CoV RNA replication or mRNA production, suggesting that imatinib inhibits a step in the replication cycle before RNA production.

Imatinib does not affect intracellular trafficking of pseudotyped viruses, MERS-CoV, or SARS-CoV. In order to achieve productive infection, SARS-CoV and MERS-CoV must be internalized by the host cell and traffic to the appropriate endosomal compartments for fusion and entry (13). We determined whether imatinib prevents trafficking of virus to early or late endosomes, thereby blocking entry of MERS-CoV and SARS-CoV, respectively (15, 16, 19). Because MERS-CoV fuses with and releases viral RNA into the cytoplasm from early endosomes and SARS-CoV fuses with and releases viral RNA into the cytoplasm from late endosomes, we assessed colocalization between endosomal trafficking markers and either pseudotyped virions (named PS/SARS-S for SARS-CoV S pseudovirions and PS/MERS-S for MERS-CoV S pseudovirions) or live SARS-CoV or MERS-CoV.

BSC and Huh-7 cells were pretreated for 1 h with imatinib, and then either control or drug-treated cells were infected with PS/SARS-S or PS/MERS-S, respectively. At 2 h postinfection for PS/SARS-S and 1 h postinfection for PS/MERS-S, cells were fixed and we performed dual-color immunofluorescence experiments to quantify colocalization for the pseudovirions and a marker for the early or late endosomes. We quantified PS/SARS-S colocalization with Lamp-1, a late endosome/lysosome marker, and colocalization of PS/MERS-S with an early endosome marker, EEA-1, by confocal microscopy using ImageJ. Our data demonstrated 37% colocalization of PS/MERS-S virions with the early endosomal marker, EEA-1, in the absence of imatinib and 47% in the presence of imatinib at 1 h postinfection (Fig. 3A). These data suggest that imatinib does not significantly affect localization of the PS/MERS-S pseudovirions to early endosomes ($P > 0.05$). We observed <10% colocalization of MERS S with Lamp-1 at several time points postinfection (data not shown), confirming that MERS-CoV pseudovirions do not traffic to late endosomes. Confocal analysis showed that ~60% of HIV-SARS-CoV S colocalized with EEA1 at 1 h postinfection in both the presence and absence of imatinib (data not shown), demonstrating that imatinib does not significantly affect early endosomal trafficking of PS/SARS-S. Similarly, the results with PS/SARS-S and the late endosomal marker Lamp-1 showed 55% colocalization in the absence and 65% colocalization in the presence of imatinib at 2 h postinfection (Fig. 3B), suggesting that imatinib does not significantly affect localization of the SARS-S pseudovirions to the late endosomes ($P > 0.05$).

Trafficking assays were performed using PS/SARS-S and PS/MERS-S to show that the pseudotyped virions were visualized in the predicted early (PS/MERS-S) and late (PS/SARS-S) endosomes (3). To ensure that this result was not due to an experimental anomaly of pseudovirus trafficking, the experiments were also performed using live virus in Vero E6 cells. Colocalization analysis showed that ~55% of SARS-CoV localized with EEA1 at 1 h postinfection and ~80% localized with Lamp1 at 2.0 h postinfection, and this was not significantly inhibited by imatinib treatment (Fig. 4A). Similarly, ~70% of MERS-CoV localized with EEA1 at 1.0 h postinfection, and this was not significantly inhibited by

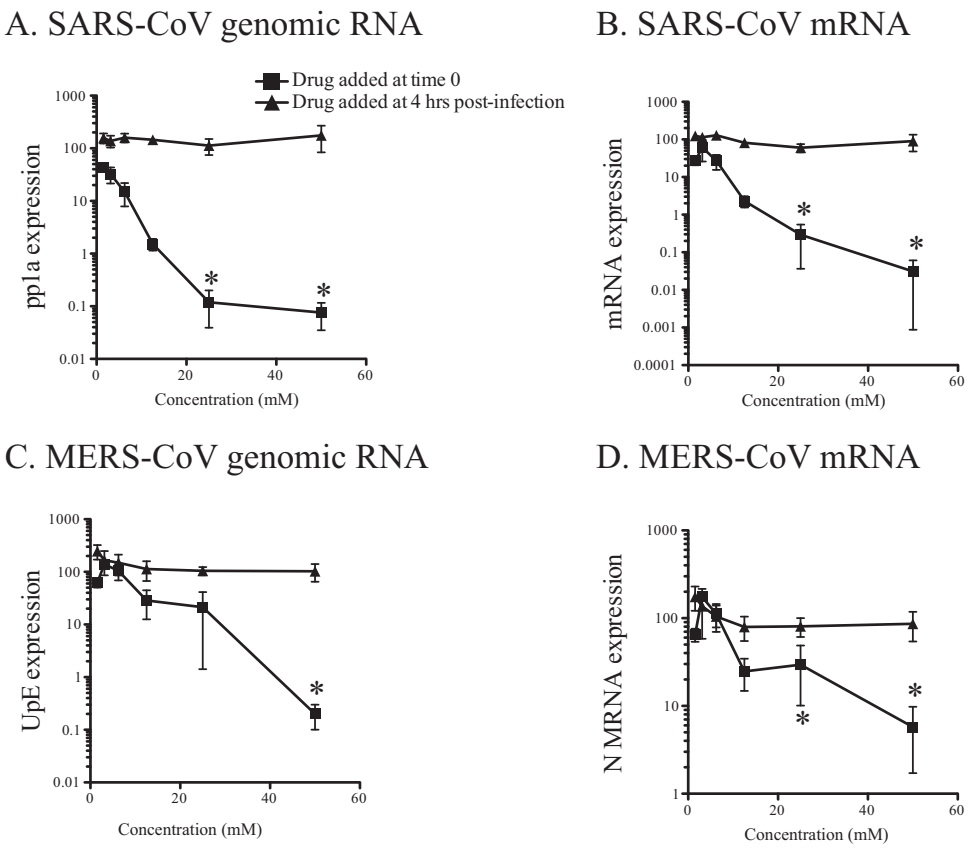

FIG 2 Imatinib inhibits SARS-CoV and MERS-CoV RNA production. Cells were treated with imatinib at the start of infection (squares) or at 4 h postinfection (triangles) with either SARS-CoV in Vero E6 (A) and Calu-3 (B) cells or MERS-CoV in Vero E6 (C) and MRC5 (D) cells. Imatinib does not significantly inhibit RNA production when added at 4 h postinfection. Data are presented as the mean ± standard deviation from 3 independent experiments. *, $P < 0.05$; **, $P < 0.01$.

imatinib treatment (Fig. 4B). Together, these data demonstrate that imatinib does not inhibit trafficking of MERS-CoV to early endosomes or of SARS-CoV to early or late endosomes.

Imatinib inhibits fusion and release of SARS-S and MERS-S pseudovirions into the cytoplasm. SARS-CoV and MERS-CoV must traffic to appropriate endosomes and then fuse with the endosomal membrane for genome delivery to the host cell cytoplasm. Our data suggest that imatinib inhibits replication of SARS-CoV and MERS-CoV but does not disrupt intracellular trafficking of either. Therefore, we next tested whether imatinib could inhibit the subsequent step in the viral life cycle, fusion of the virion to the endosomal membrane.

SARS-CoV S and MERS-CoV S pseudovirions containing a β-lactamase–Vpr chimeric protein (BlaM-vpr) incorporated into the virion were used to investigate the effect of imatinib on fusion of SARS-CoV and MERS-CoV. In this system, upon pseudovirus fusion with the endosomal membrane, BlaM is released into the cytoplasm of the infected cell. Virus fusion/entry is detected by enzymatic cleavage of CCF2, a fluorescent substrate of BlaM, delivered into the host cell cytoplasm. The β-lactam ring in CCF2 is cleaved by BlaM, which changes the emission spectrum of CCF2 from 520 nm (green) to ~450 nm (blue), allowing the fusion of the virus and endosomal membrane to be quantified using flow cytometry. Cells were treated with imatinib for 1 h before infection with BlaM-containing PS/SARS-S and PS/MERS-S. Cells were then analyzed by flow cytometry to quantify the cleavage of CCF2. Uninfected cells incubated with CCF2 show no cleavage of this substrate in the absence of BlaM (Fig. 5A, top panels). In mock-treated cells, PS/SARS-S and PS/MERS-S released BlaM into the cytoplasm after endosomal fusion, and CCF2 was readily cleaved (Fig. 5A, middle panels). Example plots of the imatinib treatment effect on PS/SARS-S and PS/MERS-S fusion are shown in the bottom panels of Fig. 5A. Upon treatment with imatinib, there was a significant reduction in CCF2 cleavage caused by PS/SARS-S (Fig. 5B) (90% reduction; $P < 0.001$) or PS/MERS-S (Fig. 5B) (80% reduction; $P < 0.001$). These data demonstrate that imatinib inhibits the fusion of PS/SARS-S and PS/MERS-S with the endosomal membrane, suggesting that imatinib blocks SARS-CoV and MERS-CoV replication by inhibiting virion fusion with the endosomal membrane, preventing nucleocapsid entry into the host cell cytoplasm and subsequent replication.

Abl2 expression enables productive SARS-CoV and MERS-CoV replication. Imatinib was designed as an Abl1 and Abl2 inhibitor to block the overactivation of Abl1/2 protein function in leukemia (23). We therefore investigated the relative role(s) of Abl1 and Abl2 in the replication of SARS-CoV and MERS-CoV using siRNA to knock down the Abl1 and Abl2 protein levels.

We achieved a significant knockdown of Abl1 (Fig. 6A) and Abl2 (Fig. 6B) in Vero E6 cells. When Abl1 mRNA was knocked down with siRNA pools and Vero E6 cells were infected with SARS-CoV or MERS-CoV, we observed no inhibition of SARS-

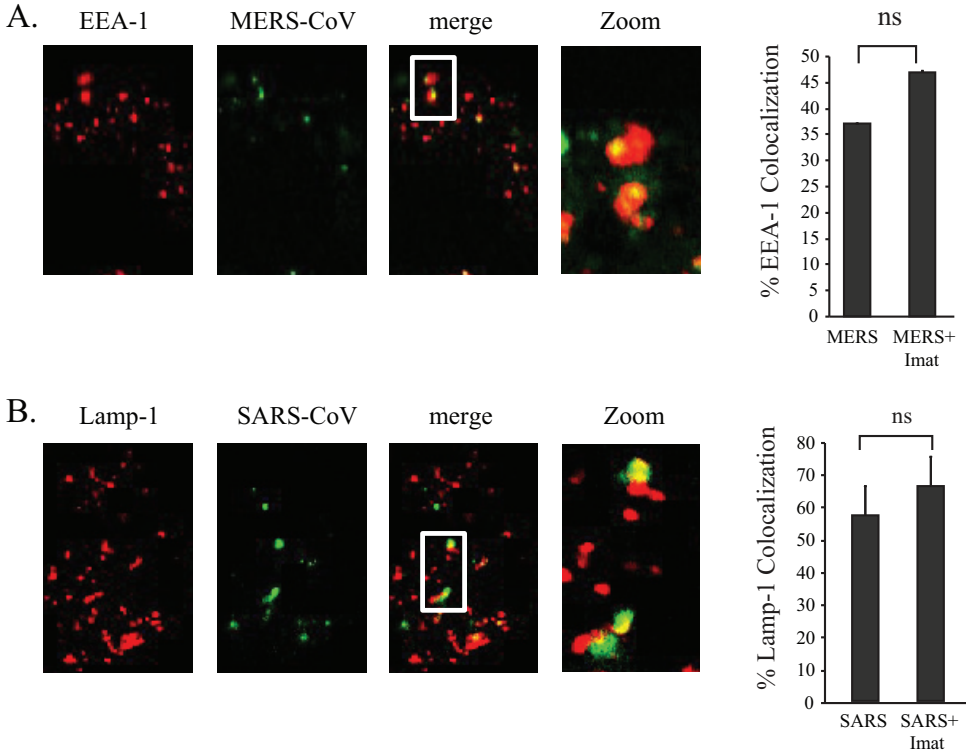

FIG 3 Imatinib does not interfere with trafficking of MERS-CoV or SARS-CoV pseudovirions to early or late endosomes, respectively. BSC1 or Huh7 cells were infected with PS/SARS-S (A) or PS/MERS-S (B), respectively, with or without a 10 μM imatinib 1-h pretreatment. For imaging colocalization of PS/MERS-S with EEA1, cells were fixed at 1 h postinfection. For imaging colocalization of PS/SARS-S with LAMP1, cells were fixed at 2 h postinfection. Graphs represent percent colocalization of virions to endosomes for 100 cells. Error bars represent mean ± standard deviation. ns, not significant.

CoV replication (Fig. 6C) or MERS-CoV replication (Fig. 6D). However, when Abl2 mRNA was knocked down, we observed a significant inhibition of SARS-CoV replication (Fig. 6C) ($P < 0.01$) and MERS-CoV replication (Fig. 6D) ($P < 0.01$). These data suggest that Abl2, but not Abl1, expression is required for efficient SARS-CoV and MERS-CoV replication.

DISCUSSION

Our previous work identified Abl kinase inhibitors as potent antagonists of coronavirus replication *in vitro* (13) but did not identify a mechanism of action. In the present study, we show how the Abl kinase antagonist imatinib inhibits SARS-CoV and MERS-CoV entry. We found that imatinib inhibited the early stages of the virus life cycle for both SARS-CoV and MERS-CoV, because when imatinib is added to cells and left for the first 4 h of infection, it inhibits release of SARS-CoV and MERS-CoV genomic RNA and production of mRNA, whereas there is significantly reduced effect when imatinib is added at 5 h postinfection. We show that imatinib does not perturb SARS-CoV or MERS-CoV virion trafficking to endosomes, suggesting that imatinib exerts its action after trafficking but prior to viral RNA expression. We show that imatinib

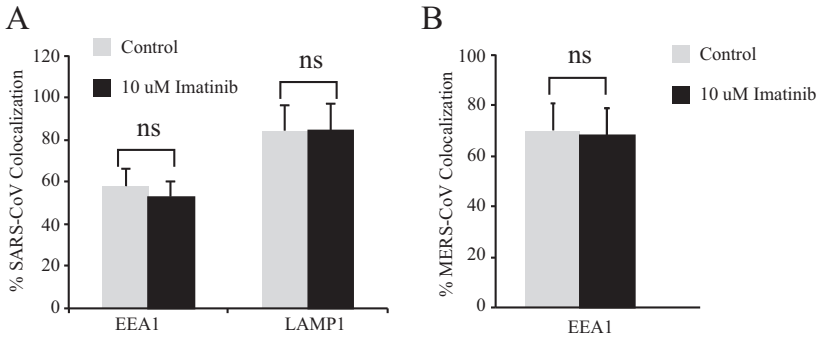

FIG 4 Imatinib does not interfere with trafficking of live MERS-CoV or SARS-CoV to early or late endosomes, respectively. Vero E6 cells were infected with live SARS-CoV (A) or MERS-CoV (B), with or without a 1-h 10 μM imatinib pretreatment. For imaging colocalization of SARS-CoV S with EEA1 or LAMP1, cells were fixed at 1 h and 2 h postinfection, respectively. For imaging colocalization of MERS-CoV S with EEA1, cells were fixed at 1 h postinfection. Graphs represent percent colocalization of virions to endosomes for 100 cells. Error bars represent mean ± standard deviation. ns, not statistically significant.

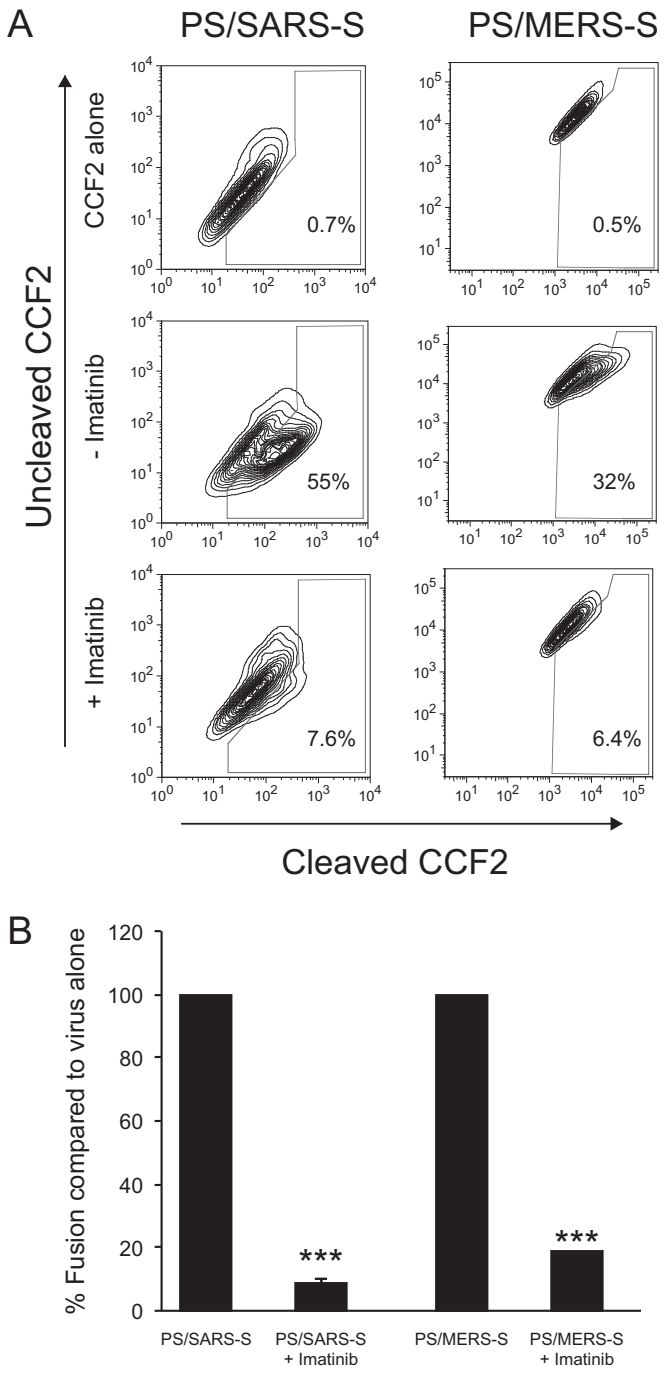

FIG 5 Imatinib inhibits SARS-CoV and MERS-CoV virion fusion with endosomal membranes. BSC1 or Huh7 cells were infected with PS/SARS-S or PS/MERS-S, respectively, with or without a 1-h 10 μM imatinib pretreatment. Cells were incubated for 3 h and then incubated in a solution containing CCF2. (A) Flow cytometry of pseudovirus entry from one representative experiment. (B) The graph shows quantification of pseudovirus entry from 3 independent experiments. Error bars represent mean ± standard deviation. ***, $P < 0.001$.

specifically inhibits viral fusion with the endosomal membrane, thereby inhibiting entry and subsequent viral genome replication. Moreover, we examined the canonical targets of imatinib, Abl1 and Abl2, and found that an siRNA-mediated knockdown of Abl2, but not Abl1, resulted in a decrease in virus replication. This suggests that imatinib inhibits virus entry through the inhibition of Abl2.

Abl kinases are ubiquitously expressed signaling kinases involved in multiple cellular signaling pathways and are important housekeeping proteins in all cell types. Other groups have reported roles for Abl kinases in replication of Ebola virus (14, 15), coxsackievirus (16), and vaccinia virus (17). Kouznetzova et al. used Ebola virus BlaM virus-like particles (VLPs) similar to those used in this present study to evaluate Ebola virus entry and identified numerous FDA-approved drugs that inhibited Ebola virus replication (15). Another study demonstrated that imatinib treatment, as well as siRNA knockdown of Abl1, prevented phosphorylation of Ebola virus VP40, which is necessary for Ebola virus virion egress from the host cell (14). Group B coxsackievirus (CVB) requires Abl1-induced actin reorganization for entry (16), as treatment of cells with imatinib prior to CVB infection causes virus accumulation at the cellular apical surface, preventing virus from reaching tight junctions, where entry normally occurs. Finally, Src family kinase activation of Abl1 and Abl2 stimulates vaccinia virus actin-based motility, suggesting a relationship between Abl kinase activity and vaccinia virus replication (17). These studies demonstrate that Abl kinases are involved in different stages of the life cycle for three different viruses. To our knowledge, this is the first report that Abl2, and not Abl1, is required for replication of a virus, in this case both SARS-CoV and MERS-CoV, and that imatinib inhibits the fusion between the coronavirus and endosomal membranes.

Abl1 and Abl2 proteins share homology in many domains but also contain distinct domains. Abl2 contains 3 proline-X-X-proline (P-X-X-P) regions, which bind SH3 domain-containing proteins or the Abl2 SH3 domain itself (24). Through these P-X-X-P regions, the Abl2 SH2 and SH3 domains fold back onto the kinase domain, keeping Abl2 in an inactive conformation (25, 26). The Abl2 conformation can switch from inactive to active upon substrate binding to either the SH2 or the SH3 domain (24). Additionally, Abl2 must be phosphorylated on 2 tyrosine residues prior to activation of its kinase domain (25, 26). The open, active conformation allows for ATP binding at the active site and subsequent kinase activity. We hypothesize that coronavirus infection leads to increased Abl2 substrate binding or that binding of specific substrates is necessary for virus entry and that this binding could result in Abl2 adopting its open, active conformation and allow for phosphorylation of downstream targets. When cells are treated with imatinib, even though Abl2 is in its open conformation, ATP is unable to bind in the active site, and as a consequence, the kinase activity of Abl2 is inhibited, preventing phosphorylation of proteins targeted by Abl2. This proposed mechanism is supported by structural analysis of dasatinib binding to Abl1, showing the kinase in the open, active conformation but unable to phosphorylate downstream targets (27). The identity of substrates and downstream targets of Abl2, in the context of coronavirus infection, is under investigation. However, Abl2 has been shown to phosphorylate proteins involved in actin cytoskeletal rearrangement, and it is possible that without Abl2 activity, through either imatinib treatment or siRNA knockdown, changes in the cytoskeleton prevent the fusion of membranes in the endosome. This is plausible considering known interactions between trafficking organelles and the cytoskeleton (28, 29). Our data suggest that coronaviruses rely on an Abl2-specific signaling event and that this may play a role in trafficking or activation of specific cytoskeletal or endosomal

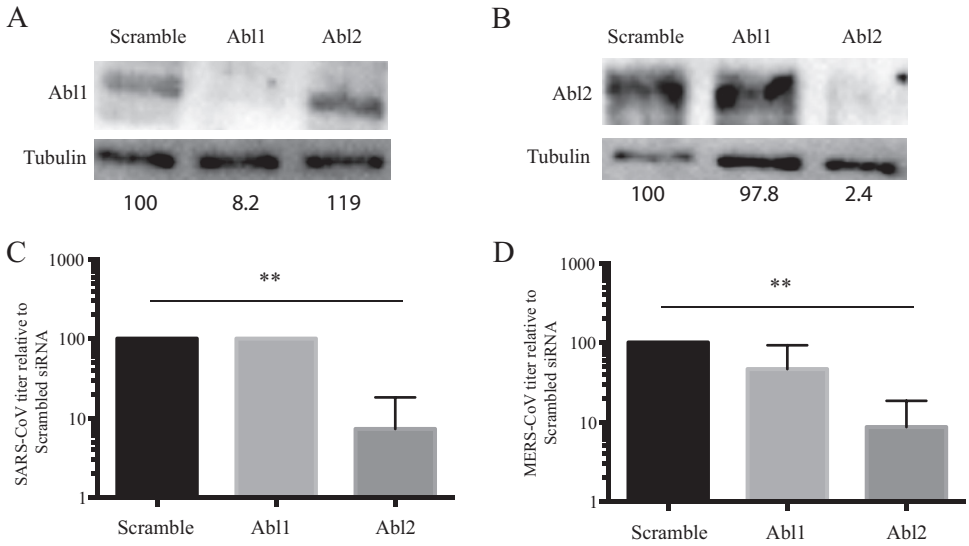

FIG 6 Specific knockdown of Abl2, and not Abl1, significantly inhibits MERS-CoV and SARS-CoV replication. (A and B) Specific knockdown of ABl1 (A) and Abl2 (B) was achieved in Vero E6 cells. Numbers under bands are the percentage of each knocked down protein relative to scrambled siRNA, normalized for tubulin levels. (C and D) Knockdown of Abl2, and not Abl1, specifically inhibits production of infectious SARS-CoV (C) and MERS-CoV (D) from transfected cells. Data in panels C and D are presented as mean ± standard deviation from 3 independent experiments. **, $P < 0.01$.

proteins, which in turn lead to cleavage of coronavirus S proteins in the lumen of endosomes, resulting in virion/endosome membrane fusion. The precise mechanism of the Abl2 effect on SARS-CoV and MERS-CoV virion fusion is under investigation.

SARS-CoV and MERS-CoV go through a staged entry process involving endocytosis of virions after receptor binding, intracellular trafficking of virions to late or early endosomes, respectively, and fusion of the virion membrane with the endosomal membrane to deposit the nucleocapsid into the cytoplasm. Alternatively, others have shown cleavage of coronavirus S by the type II transmembrane serine protease (TTSP) TMPRSS2, a surface-expressed serine protease that was shown to activate diverse coronaviruses in cell culture by cleavage of the S protein on the surface of the virion, leading to enhanced entry of the virus into a cell (30–35). Treating cells with a serine protease inhibitor, camostat, which inhibits TMPRSS2 activity, partially blocks coronavirus entry *in vitro*, as did a cathepsin inhibitor, but both together completely block virus entry and replication (36). Therefore, imatinib and Abl2 could inhibit TMPRSS2 function, localization, or activity. Although imatinib and Abl2 have not been linked to TMPRSS2, they may affect TMPRSS2 function in the cell and therefore could inhibit virus entry and spread.

Imatinib has been tolerated well for long-term use in chronic myeloid leukemia (CML) patients (37). Dasatinib, a second-generation Abl kinase inhibitor, has been shown to be significantly more effective than imatinib at targeting cells expressing BCR-Abl and also very effective against cells expressing imatinib-resistant BCR-Abl mutants, and it is safe for long-term use in human patients (38). As an antiviral, treatment would likely be for short periods of time, for example, when traveling to an area of endemicity or after exposure to an infected person or persons. The concentration of imatinib needed to inhibit SARS-CoV and MERS-CoV in this current study, though high, is within the range previously reported for Ebola virus, CVB, and vaccinia virus (14–17). The need for this high concentration of drug could be due to experimental factors of cell line resistance or the amount of virus used in these experiments. Further studies *in vivo* are warranted to identify dosing regimens for SARS-CoV and MERS-CoV mouse models.

In this study, we have demonstrated that drugs screened *in vitro* for anticoronavirus activity can be characterized as to their specific effect on coronavirus replication and be used to identify novel host pathways required for coronavirus replication. In addition, we identified Abl2 as a novel host cell protein involved in coronavirus virion replication and hypothesize that Abl2 is required for virion fusion at the endosomal membrane by a mechanism that is under investigation. The repurposing of FDA-approved compounds, such as imatinib, provides a rich source of novel therapeutics for treatment of emerging viruses and to identify additional target pathways for future drug development.

ACKNOWLEDGMENTS

We thank Mayra Garcia, Daniel Kalman, Carolyn Coyne, and Carolyn Machamer for helpful discussion and reagents.

This project has been funded in part by a supplement to NIH RO1 AI095569 (M.B.F.), NIH R21AI103601 (J.M.W.), NIH R01AI114776 (J.M.W.), and F32 AI118303 (J.M.S.).

FUNDING INFORMATION

This work, including the efforts of Matthew B. Frieman, was funded by HHS | NIH | National Institute of Allergy and Infectious Diseases (NIAID) (AI095569). This work, including the efforts of Judith Miriam White, was funded by HHS | NIH | National Institute of Allergy and Infectious Diseases (NIAID) (R21AI103601 and R01AI114776). This work, including the efforts of Jeanne M. Sisk, was funded by HHS | NIH | National Institute of Allergy and Infectious Diseases (NIAID) (AI118303).

REFERENCES

1. **Fehr AR, Perlman S.** 2015. Coronaviruses: an overview of their replication and pathogenesis. Methods Mol Biol **1282:**1–23. http://dx.doi.org/10.1007/978-1-4939-2438-7_1.

2. **Simmons G, Gosalia DN, Rennekamp AJ, Reeves JD, Diamond SL, Bates P.** 2005. Inhibitors of cathepsin L prevent severe acute respiratory syndrome coronavirus entry. Proc Natl Acad Sci U S A **102:**11876–11881. http://dx.doi.org/10.1073/pnas.0505577102.
3. **Burkard C, Verheije MH, Wicht O, van Kasteren SI, van Kuppeveld FJ, Haagmans BL, Pelkmans L, Rottier PJ, Bosch BJ, de Haan CA.** 2014. Coronavirus cell entry occurs through the endo-/lysosomal pathway in a proteolysis-dependent manner. PLoS Pathog **10:**e1004502. http://dx.doi.org/10.1371/journal.ppat.1004502.
4. **Tan EL, Ooi EE, Lin CY, Tan HC, Ling AE, Lim B, Stanton LW.** 2004. Inhibition of SARS coronavirus infection in vitro with clinically approved antiviral drugs. Emerg Infect Dis **10:**581–586. http://dx.doi.org/10.3201/eid1004.030458.
5. **Sirois S, Wei DQ, Du Q, Chou KC.** 2004. Virtual screening for SARS-CoV protease based on KZ7088 pharmacophore points. J Chem Infect Comput Sci **44:**1111–1122. http://dx.doi.org/10.1021/ci034270n.
6. **Chou KC, Wei DQ, Zhong WZ.** 2003. Binding mechanism of coronavirus main proteinase with ligands and its implication to drug design against SARS. Biochem Biophys Res Commun **308:**148–151. http://dx.doi.org/10.1016/S0006-291X(03)01342-1.
7. **Anand K, Ziebuhr J, Wadhwani P, Mesters JR, Hilgenfeld R.** 2003. Coronavirus main proteinase (3CLpro) structure: basis for design of anti-SARS drugs. Science **300:**1763–1767. http://dx.doi.org/10.1126/science.1085658.
8. **Hertzig T, Scandella E, Schelle B, Ziebuhr J, Siddell SG, Ludewig B, Thiel V.** 2004. Rapid identification of coronavirus replicase inhibitors using a selectable replicon RNA. J Gen Virol **85:**1717–1725. http://dx.doi.org/10.1099/vir.0.80044-0.
9. **Adedeji AO, Singh K, Calcaterra NE, DeDiego ML, Enjuanes L, Weiss S, Sarafianos SG.** 2012. Severe acute respiratory syndrome coronavirus replication inhibitor that interferes with the nucleic acid unwinding of the viral helicase. Antimicrob Agents Chemother **56:**4718–4728. http://dx.doi.org/10.1128/AAC.00957-12.
10. **Huang JD, Zheng BJ, Sun HZ.** 2008. Helicases as antiviral drug targets. Hong Kong Med J **14**(Suppl 4)**:**S36–S38.
11. **Adedeji AO, Singh K, Sarafianos SG.** 2012. Structural and biochemical basis for the difference in the helicase activity of two different constructs of SARS-CoV helicase. Cell Mol Biol (Noisy-le-grand) **58:**114–121.
12. **Wong SS, Yuen KY.** 2008. The management of coronavirus infections with particular reference to SARS. J Antimicrob Chemother **62:**437–441. http://dx.doi.org/10.1093/jac/dkn243.
13. **Dyall J, Coleman CM, Hart BJ, Venkataraman T, Holbrook MR, Kindrachuk J, Johnson RF, Olinger GG, Jr, Jahrling PB, Laidlaw M, Johansen LM, Lear CM, Glass PJ, Hensley LE, Frieman MB.** 2014. Repurposing of clinically developed drugs for treatment of Middle East respiratory coronavirus infection. Antimicrob Agents Chemother **58:**4885–4893. http://dx.doi.org/10.1128/AAC.03036-14.
14. **Garcia M, Cooper A, Shi W, Bornmann W, Carrion R, Kalman D, Nabel GJ.** 2012. Productive replication of Ebola virus is regulated by the c-Abl1 tyrosine kinase. Sci Transl Med **4:**123ra124.
15. **Kouznetsova J, Sun W, Martinez-Romero C, Tawa G, Shinn P, Chen CZ, Schimmer A, Sanderson P, McKew JC, Zheng W, Garcia-Sastre A.** 2014. Identification of 53 compounds that block Ebola virus-like particle entry via a repurposing screen of approved drugs. Emerg Microbes Infect **3:**e84. http://dx.doi.org/10.1038/emi.2014.88.
16. **Coyne CB, Bergelson JM.** 2006. Virus-induced Abl and Fyn kinase signals permit coxsackievirus entry through epithelial tight junctions. Cell **124:**119–131. http://dx.doi.org/10.1016/j.cell.2005.10.035.
17. **Newsome TP, Weisswange I, Frischknecht F, Way M.** 2006. Abl collaborates with Src family kinases to stimulate actin-based motility of vaccinia virus. Cell Microbiol **8:**233–241. http://dx.doi.org/10.1111/j.1462-5822.2005.00613.x.
18. **Roberts A, Deming D, Paddock CD, Cheng A, Yount B, Vogel L, Herman BD, Sheahan T, Heise M, Genrich GL, Zaki SR, Baric R, Subbarao K.** 2007. A mouse-adapted SARS-coronavirus causes disease and mortality in BALB/c mice. PLoS Pathog **3:**e5. http://dx.doi.org/10.1371/journal.ppat.0030005.
19. **Frieman M, Yount B, Agnihothram S, Page C, Donaldson E, Roberts A, Vogel L, Woodruff B, Scorpio D, Subbarao K, Baric RS.** 2012. Molecular determinants of severe acute respiratory syndrome coronavirus pathogenesis and virulence in young and aged mouse models of human disease. J Virol **86:**884–897. http://dx.doi.org/10.1128/JVI.05957-11.
20. **Coleman CM, Frieman MB.** 2015. Growth and quantification of MERS-CoV infection. Curr Protoc Microbiol **37:**2–15. http://dx.doi.org/10.1002/9780471729259.mc15e02s37.
21. **Taylor JK, Coleman CM, Postel S, Sisk JM, Bernbaum JG, Venkatarajan T, Sundberg EJ, Frieman MB.** 2015. Severe acute respiratory syndrome coronavirus ORF7a inhibits bone marrow stromal antigen 2 virion tethering through a novel mechanism of glycosylation interference. J Virol **89:**11820–11833. http://dx.doi.org/10.1128/JVI.02274-15.
22. **Mingo RM, Simmons JA, Shoemaker CJ, Nelson EA, Schornberg KL, D'Souza RS, Casanova JE, White JM.** 2015. Ebola virus and severe acute respiratory syndrome coronavirus display late cell entry kinetics: evidence that transport to NPC1+ endolysosomes is a rate-defining step. J Virol **89:**2931–2943. http://dx.doi.org/10.1128/JVI.03398-14.
23. **Greuber EK, Smith-Pearson P, Wang J, Pendergast AM.** 2013. Role of ABL family kinases in cancer: from leukaemia to solid tumours. Nat Rev Cancer **13:**559–571. http://dx.doi.org/10.1038/nrc3563.
24. **Colicelli J.** 2010. ABL tyrosine kinases: evolution of function, regulation, and specificity. Sci Signal **3:**re6. http://dx.doi.org/10.1126/scisignal.3139re6.
25. **Bradley WD, Koleske AJ.** 2009. Regulation of cell migration and morphogenesis by Abl-family kinases: emerging mechanisms and physiological contexts. J Cell Sci **122:**3441–3454. http://dx.doi.org/10.1242/jcs.039859.
26. **Wang J, Pendergast AM.** 2015. The emerging role of ABL kinases in solid tumors. Trends Cancer **1:**110–123. http://dx.doi.org/10.1016/j.trecan.2015.07.004.
27. **Tokarski JS, Newitt JA, Chang CY, Cheng JD, Wittekind M, Kiefer SE, Kish K, Lee FY, Borzillerri R, Lombardo LJ, Xie D, Zhang Y, Klei HE.** 2006. The structure of Dasatinib (BMS-354825) bound to activated ABL kinase domain elucidates its inhibitory activity against imatinib-resistant ABL mutants. Cancer Res **66:**5790–5797. http://dx.doi.org/10.1158/0008-5472.CAN-05-4187.
28. **Seabra MC, Coudrier E.** 2004. Rab GTPases and myosin motors in organelle motility. Traffic **5:**393–399. http://dx.doi.org/10.1111/j.1398-9219.2004.00190.x.
29. **Sandilands E, Frame MC.** 2008. Endosomal trafficking of Src tyrosine kinase. Trends Cell Biol **18:**322–329. http://dx.doi.org/10.1016/j.tcb.2008.05.004.
30. **Glowacka I, Bertram S, Muller MA, Allen P, Soilleux E, Pfefferle S, Steffen I, Tsegaye TS, He Y, Gnirss K, Niemeyer D, Schneider H, Drosten C, Pohlmann S.** 2011. Evidence that TMPRSS2 activates the severe acute respiratory syndrome coronavirus spike protein for membrane fusion and reduces viral control by the humoral immune response. J Virol **85:**4122–4134. http://dx.doi.org/10.1128/JVI.02232-10.
31. **Bertram S, Glowacka I, Muller MA, Lavender H, Gnirss K, Nehlmeier I, Niemeyer D, He Y, Simmons G, Drosten C, Soilleux EJ, Jahn O, Steffen I, Pohlmann S.** 2011. Cleavage and activation of the severe acute respiratory syndrome coronavirus spike protein by human airway trypsin-like protease. J Virol **85:**13363–13372. http://dx.doi.org/10.1128/JVI.05300-11.
32. **Bertram S, Dijkman R, Habjan M, Heurich A, Gierer S, Glowacka I, Welsch K, Winkler M, Schneider H, Hofmann-Winkler H, Thiel V, Pohlmann S.** 2013. TMPRSS2 activates the human coronavirus 229E for cathepsin-independent host cell entry and is expressed in viral target cells in the respiratory epithelium. J Virol **87:**6150–6160. http://dx.doi.org/10.1128/JVI.03372-12.
33. **Leow MK.** 2013. Correlating cell line studies with tissue distribution of DPP4/TMPRSS2 and human biological samples may better define the viral tropism of MERS-CoV. J Infect Dis **208:**1350–1351. http://dx.doi.org/10.1093/infdis/jit330.
34. **Gierer S, Bertram S, Kaup F, Wrensch F, Heurich A, Kramer-Kuhl A, Welsch K, Winkler M, Meyer B, Drosten C, Dittmer U, von Hahn T, Simmons G, Hofmann H, Pohlmann S.** 2013. The spike protein of the emerging betacoronavirus EMC uses a novel coronavirus receptor for entry, can be activated by TMPRSS2, and is targeted by neutralizing antibodies. J Virol **87:**5502–5511. http://dx.doi.org/10.1128/JVI.00128-13.
35. **Simmons G, Zmora P, Gierer S, Heurich A, Pohlmann S.** 2013. Proteolytic activation of the SARS-coronavirus spike protein: cutting enzymes at the cutting edge of antiviral research. Antiviral Res **100:**605–614. http://dx.doi.org/10.1016/j.antiviral.2013.09.028.
36. **Shirato K, Kawase M, Matsuyama S.** 2013. Middle East respiratory syndrome coronavirus infection mediated by the transmembrane serine

protease TMPRSS2. J Virol **87:**12552–12561. http://dx.doi.org/10.1128/JVI.01890-13.

37. **Kalmanti L, Saussele S, Lauseker M, Muller MC, Dietz CT, Heinrich L, Hanfstein B, Proetel U, Fabarius A, Krause SW, Rinaldetti S, Dengler J, Falge C, Oppliger-Leibundgut E, Burchert A, Neubauer A, Kanz L, Stegelmann F, Pfreundschuh M, Spiekermann K, Scheid C, Pfirrmann M, Hochhaus A, Hasford J, Hehlmann R.** 2015. Safety and efficacy of imatinib in CML over a period of 10 years: data from the randomized CML-study IV. Leukemia **29:**1123–1132. http://dx.doi.org/10.1038/leu.2015.36.
38. **O'Hare T, Walters DK, Stoffregen EP, Sherbenou DW, Heinrich MC, Deininger MW, Druker BJ.** 2005. Combined Abl inhibitor therapy for minimizing drug resistance in chronic myeloid leukemia: Src/Abl inhibitors are compatible with imatinib. Clin Cancer Res **11:**6987–6993. http://dx.doi.org/10.1158/1078-0432.CCR-05-0622.